

# Constraints on decaying early modified gravity from cosmological observations

Nelson A. Lima,<sup>\*</sup> Vanessa Smer-Barreto,<sup>†</sup> and Lucas Lombriser<sup>‡</sup>

*Institute for Astronomy, University of Edinburgh,  
Royal Observatory, Blackford Hill, Edinburgh EH9 3HJ, United Kingdom*  
(Received 20 March 2016; published 4 October 2016)

Most of the information on our cosmos stems from either late-time observations or the imprint of early-time inhomogeneities on the cosmic microwave background. We explore to what extent early modifications of gravity, which become significant after recombination but then decay toward the present, can be constrained by current cosmological observations. For the evolution of the gravitational modification, we adopt the decaying mode of a hybrid metric-Palatini  $f(\mathcal{R})$  gravity model which is designed to reproduce the standard cosmological background expansion history and due to the decay of the modification is naturally compatible with Solar System tests. We embed the model in the effective field theory description of Horndeski scalar-tensor gravity with an early-time decoupling of the gravitational modification. Since the quasistatic approximation for the perturbations in the model breaks down at high redshifts, where modifications remain relevant, we introduce a computationally efficient correction to describe the evolution of the scalar field fluctuation in this regime. We compare the decaying early-time modification against geometric probes and recent Planck measurements and find no evidence for such effects in the observations. Current data constrains the scalar field value at  $|f_{\mathcal{R}}(z = z_{\text{on}})| \lesssim 10^{-2}$  for modifications introduced at redshifts  $z_{\text{on}} \sim (500\text{--}1000)$  with the present-day value  $|f_{\mathcal{R}0}| \lesssim 10^{-8}$ . Finally, we comment on constraints that will be achievable with future 21-cm surveys and gravitational wave experiments.

DOI: [10.1103/PhysRevD.94.083507](https://doi.org/10.1103/PhysRevD.94.083507)

## I. INTRODUCTION

Lovelock's theorem on the uniqueness of Einstein's gravitational field equations does not apply in the presence of higher than second-order derivatives of the metric, additional gravitational degrees of freedom, extra dimensions, or other unconventional properties that a more fundamental theory of gravity may be endowed with. Such a theory could give rise to new phenomenological aspects at different scales and epochs in time that may potentially be observable and can be tested using existent modified gravity theories.

Einstein's theory of general relativity (GR) has been well tested in the Solar System, where, however, potential large-scale deviations may be suppressed due to screening effects [1–3]. There is now a complementary effort in obtaining competitive constraints on larger scales, with a surge of surveys that will significantly improve our knowledge of the cosmological regime, such as the Dark Energy Survey [4], the extended Baryon Oscillation Spectroscopic Survey [5] and the Euclid survey [6] (for a review on cosmological tests of gravity see [2]).

Much of the interest in modified gravity theories has arisen in the search for alternative explanations for the observed late-time accelerated expansion of our Universe

[7–10], possibly avoiding the fine-tuning problem of the cosmological constant  $\Lambda$  adopted in the standard model of cosmology  $\Lambda$  cold dark matter (CDM) (for reviews on modified gravity, the cosmological constant, and dark energy see [1–3,11]). However, in Ref. [12] it has recently been shown that scalar-tensor theories of gravity such as Brans-Dicke [13], Galileon [14], and  $f(R)$  gravity [15], or any other models embedded in the Horndeski action [16], cannot yield an observationally compatible self-acceleration effect due to modified gravity that is genuinely different from  $\Lambda$  or dark energy, unless the cosmological speed of gravitational waves differs substantially from the speed of light. While such a deviation is unlikely [17], modified gravity theories are nevertheless relevant to test gravity and understand how it acts across all scales and epochs in cosmic time.

However, given the original interest in cosmic acceleration, the study of modified gravity has predominantly focused on late-time effects with a recovery of GR at high redshifts. Hence, early-time modifications have, so far, evaded a thorough investigation and when they have been studied (e.g., [18,19]), their effects at early times have not been clearly separated from their late-time effects. The missing analysis of early-time modifications and their impact on cosmological observables constitutes a gap in our current understanding of the gravitational processes at work and we lack a consistent quantitative analysis of the constraining power that current (and future) cosmological

<sup>\*</sup>ndal@roe.ac.uk

<sup>†</sup>vsm@roe.ac.uk

<sup>‡</sup>llo@roe.ac.uk

surveys have over this regime of gravity. Generally, the assumption of GR at early times without a test against alternatives is a strong extrapolation from its exclusive validity in the late-time Solar System region (or even from late-time cosmology). This investigation is also important to quantify the improvement on our current understanding of the cosmological model that can be expected with future surveys such as 21-cm intensity mapping (see, e.g., [20] for expected dark energy constraints), the use of gravitational waves as standard sirens at high redshifts, or constraints from surveys such as the Square Kilometer Array on the horizon [21].

In this paper, we explore to what extent modifications of gravity that may arise after recombination and decay toward the present can be constrained with current cosmological observations that stem either from their impact on the late-time large-scale structure or changes in the imprint of early-time inhomogeneities on the cosmic microwave background. For this purpose, we adopt the decaying mode of a hybrid metric-Palatini gravity model, which enables us to separate early- from late-time effects. We then compare the constraining power of future 21-cm intensity mapping and standard sirens to these current constraints.

The outline of the paper is as follows. In Sec. II A, we introduce and discuss the early-time decaying modified gravity model adopted for our analysis. In Sec. II B, we reproduce its linearly perturbed modified Einstein equations in the Newtonian gauge. We explicitly show how the breakdown of the quasistatic approximation for the evolution of the scalar field fluctuation occurs at high redshifts. This failure motivates an analytic correction to the quasistatic approximation to accurately describe the evolution of the slip between the metric potentials in this high-curvature regime. In Secs. II C and II D, we describe an embedding of this gravitational modification in the effective field theory of Horndeski scalar-tensor gravity (reviewed in Ref. [22]) with a postrecombination high-redshift decoupling of the modification to comply with stringent high-curvature constraints from the cosmic microwave background (CMB). In Sec. III, we infer constraints on the early-time decaying modified gravity model using current cosmological observations. Lastly, in Sec. IV we conclude with some final thoughts and remarks, also providing an outlook for future cosmological constraints on the model. For completeness, in the appendixes we provide details on our numerical computations and approximations adopted to describe oscillations in the scalar field fluctuations.

## II. A DECAYING EARLY MODIFICATION OF GRAVITY

The main purpose of this work is to explore constraints on early modified gravity, with modifications from GR arising at high redshifts and being suppressed as we approach the present time. We start by describing the

general dynamics of the test model we will embed in Horndeski theory: the hybrid metric-Palatini  $f(\mathcal{R})$  gravity, where the metric and the connection are considered as independent variables.

Note that while metric  $f(R)$  theory, where the connection is not independent, is much more frequently adopted as toy model to study modifications of gravity, and also possesses a decaying mode [23], it naturally predicts a 4/3 enhancement of the effective gravitational coupling in unscreened observables at late times and small scales. There always exists a small enough object in a late-time, low-density environment that is not screened and hence exhibits a modified gravity effect that could potentially be used to constrain the modification of, for instance, a dwarf galaxy in a void [24]. Similarly, an up-weighting of low-density regions in statistical observations of the large-scale structure can be used to effectively unscreen the modifications [25]. Hybrid metric-Palatini gravity evades these constraints as the unscreened effective gravitational coupling itself tends to the Newtonian value at late times (this argument will be explained in more detail in Sec. II B 1).

### A. Hybrid metric-Palatini gravity

The four-dimensional action describing the hybrid metric-Palatini gravity is given by [26]

$$S = \frac{1}{2\kappa^2} \int d^4x \sqrt{-g} [R + f(\mathcal{R})] + S_m, \quad (1)$$

where  $\kappa^2 = 8\pi G$  and we set  $c = 1$ .  $S_m$  is the standard matter action,  $R$  is the metric Ricci scalar and  $\mathcal{R} = g^{\mu\nu} \mathcal{R}_{\mu\nu}$  is the Palatini curvature. The latter is defined in terms of the metric elements,  $g^{\mu\nu}$ , and a torsionless independent connection,  $\hat{\Gamma}$ , through

$$\mathcal{R} \equiv g^{\mu\nu} (\hat{\Gamma}_{\mu\nu,\alpha}^\alpha - \hat{\Gamma}_{\mu\alpha,\nu}^\alpha + \hat{\Gamma}_{\alpha\lambda}^\alpha \hat{\Gamma}_{\mu\nu}^\lambda - \hat{\Gamma}_{\mu\lambda}^\alpha \hat{\Gamma}_{\alpha\nu}^\lambda). \quad (2)$$

For a statistically spatially homogeneous and isotropic universe with the Friedmann-Robertson-Walker metric,  $ds^2 = -dt^2 + a^2(t)d\vec{x}^2$ , the modified Einstein equations and the dynamical hybrid metric scalar field equation yield the modified Friedmann equations and background scalar field equation [26,27]:

$$3H^2 = \frac{1}{1+f_{\mathcal{R}}} \left[ \kappa^2 \rho - 3H\dot{f}_{\mathcal{R}} - \frac{3\dot{f}_{\mathcal{R}}^2}{4f_{\mathcal{R}}} + \frac{\mathcal{R}f_{\mathcal{R}} - f(\mathcal{R})}{2} \right], \quad (3)$$

$$2\dot{H} = \frac{1}{1+f_{\mathcal{R}}} \left[ -\kappa^2(\rho + p) + H\dot{f}_{\mathcal{R}} - \dot{f}_{\mathcal{R}} + \frac{3\dot{f}_{\mathcal{R}}^2}{2f_{\mathcal{R}}} \right], \quad (4)$$

$$\ddot{\mathcal{R}} = -\frac{1}{f_{\mathcal{R}\mathcal{R}}} \left[ \dot{\mathcal{R}}^2 \left( f_{\mathcal{R}\mathcal{R}\mathcal{R}} - \frac{f_{\mathcal{R}\mathcal{R}}^2}{2f_{\mathcal{R}}} \right) + 3H\dot{\mathcal{R}}f_{\mathcal{R}\mathcal{R}} + \frac{f_{\mathcal{R}}}{3} [\mathcal{R}(f_{\mathcal{R}} - 1) - 2f(\mathcal{R})] - \kappa^2 \frac{f_{\mathcal{R}}}{3} T \right], \quad (5)$$

where dots denote derivatives with respect to physical time,  $t$ ,  $H = \dot{a}/a$  is the Hubble parameter, and  $f_{\mathcal{R}}$  is the extra scalar degree of freedom introduced in the model. Here,  $f_{\mathcal{R}}$ ,  $f_{\mathcal{R}\mathcal{R}}$ ,  $f_{\mathcal{R}\mathcal{R}\mathcal{R}}$  denote the first, second, and third derivatives of  $f(\mathcal{R})$  with respect to  $\mathcal{R}$ . Equations (3), (4), and (5) constitute a closed set of differential equations that determines the background evolution for a specified  $f(\mathcal{R})$ . Note that we recover the standard Friedmann equations of  $\Lambda$ CDM in the limit of  $f_{\mathcal{R}} \rightarrow 0$ .

Lastly, it is useful to write the effective mass of the additional scalar degree of freedom, which is given by [26,27]

$$m_{f_{\mathcal{R}}}^2 = \frac{2V(f_{\mathcal{R}}) - V_{f_{\mathcal{R}}} - f_{\mathcal{R}}(1 + f_{\mathcal{R}})V_{f_{\mathcal{R}}f_{\mathcal{R}}}}{3}, \quad (6)$$

where  $V(f_{\mathcal{R}}) = \mathcal{R}f_{\mathcal{R}} - f(\mathcal{R})$  is the scalar field potential, defined in the scalar-tensor formulation of the hybrid metric-Palatini theory.

The hybrid metric-Palatini theory avoids the well-known instabilities in the pure Palatini approach [28–30] by providing a propagating additional scalar degree of freedom that can modify gravity across all scales due to its light, long-range interacting nature [26,27,31,32]. Furthermore, it does not require the effective mass of the scalar field to be massive in order to be viable on small scales, as this is assured as long as the amplitude of the scalar field remains small [27], which our designer model naturally guarantees.

### 1. Designer $f(\mathcal{R})$ model

We briefly review the designer hybrid metric-Palatini model that we will adopt to describe the evolution of the decaying early modification of gravity and its observational constraints in Sec. III. This model was first introduced in Ref. [33], and it allows one to retrieve a family of  $f(\mathcal{R})$  functions that produce a background evolution indistinguishable to  $\Lambda$ CDM from solving the second-order differential equation

$$f_{\mathcal{R}}'' + f_{\mathcal{R}}' \left( \frac{E'}{2E} - 1 \right) + f_{\mathcal{R}} \frac{E'}{E} - \frac{3f_{\mathcal{R}}^2}{2f_{\mathcal{R}}} = 0, \quad (7)$$

where here and throughout the rest of the paper primes represent derivatives with respect to  $\ln a$ . Equation (7) is obtained from setting the effective equation of state  $w_{\text{eff}}$  equal to  $-1$ . The background evolution is fixed through  $E(a) \equiv H^2/H_0^2 = \Omega_{\text{m}}a^{-3} + \Omega_{\text{r}}a^{-4} + \Omega_{\text{eff}}a^3 \int_a^1 (1+w_{\text{eff}})d \ln a$ . In a flat Universe,  $\Omega_{\text{eff}} = 1 - \Omega_{\text{m}} - \Omega_{\text{r}}$  and, for  $w_{\text{eff}} = -1$ , one recovers a  $\Lambda$ CDM-like background cosmology. The

initial conditions for solving Eq. (7) are set at an initial scale factor,  $a_i = (1 + z_i)^{-1} \ll 1$ , by [33]

$$f_{\mathcal{R}i} = C_1 a_i^{-a_{\text{aux}}} \left[ \cosh \left( \frac{1}{2} [\ln a_i + C_2] \sqrt{d} \right) \right]^{-2}, \quad (8)$$

$$f'_{\mathcal{R}i} = -C_1 \frac{a_i^{-a_{\text{aux}}}}{\cosh(\dots)^2} [a_{\text{aux}} + \sqrt{d} \tanh(\dots)], \quad (9)$$

where  $d = a_{\text{aux}}^2 - 2b$ ,  $a_{\text{aux}} = (5 + 6r_i)/(2 + 2r_i)$ , and  $b = (3 + 4r_i)/(1 + r_i)$ , with  $r_i = \Omega_{\gamma}(\Omega_{\text{m}}a_i)^{-1}$ . The dotted arguments of the hyperbolic functions refer to the same argument as in the hyperbolic cosine in Eq. (8). Throughout the paper we fix  $C_2$  to a large value in order for the absolute value of the hyperbolic tangent to be close to unity.  $C_1$  is then fixed by choosing a value for  $f_{\mathcal{R}i} \equiv f_{\mathcal{R}}(z = z_i)$ . Hence, one then just has to numerically evolve the model using Eq. (7), and make use of the background equations to recover further quantities of interest, such as  $f(\mathcal{R})$ , at each step of the iteration.

In Fig. 1 we plot the evolution of the absolute value of  $f_{\mathcal{R}}$  as a function of the scale factor for different initial values  $f_{\mathcal{R}i}$  set at a redshift  $z_i = 1000$ . The scalar field  $f_{\mathcal{R}}$  decays with time and is strongly suppressed as we approach  $a \rightarrow 1$ . In Sec. III it will become evident that due to this suppression,  $f(\mathcal{R})$  behaves like a decaying early-modified gravity model that satisfies Solar System constraints [26].

Having a hybrid metric-Palatini model that recovers a  $\Lambda$ CDM-like background evolution allows us to separate the modifications introduced between linear perturbations from background effects. Possible deviations at the background level from  $\Lambda$ CDM for other  $f(\mathcal{R})$  functions have already been tested against observations in Ref. [34], where constraints on the initial value of the scalar field  $f_{\mathcal{R}i}$  at

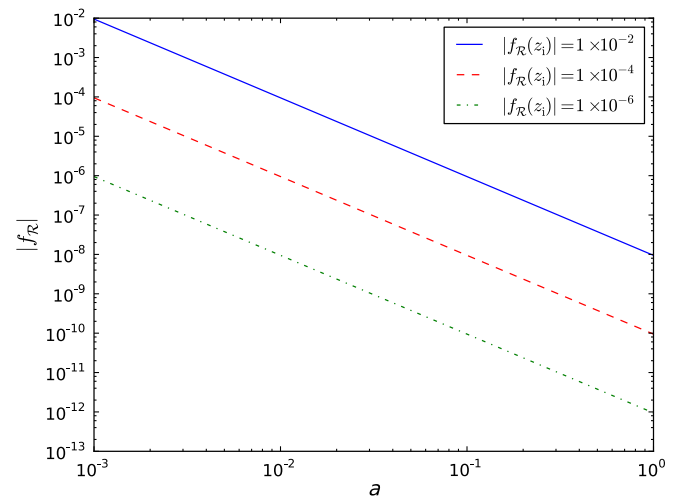


FIG. 1. Evolution of the absolute value of the extra scalar degree of freedom introduced in  $f(\mathcal{R})$  theories,  $f_{\mathcal{R}}$ , as a function of the scale factor,  $a$ , with  $z_i = 1000$ . We have fixed  $\Omega_{\text{m}} = 0.30$  for illustration.

very early times ( $z_i \sim 10^8$ ) were obtained, restricting its maximum amplitude to an absolute value of  $1 \times 10^{-2}$ . Considering how hybrid metric-Palatini models couple to the gravitational sector through a factor of  $(1 + \phi)$ , this constrained the maximum variation of the effective gravitational constant  $G_{\text{eff}}$  in the background evolution to 1% of its Newtonian value. This result is compatible with constraints on  $G_{\text{eff}}$  from big bang nucleosynthesis [35].

Modifications introduced in the linear cosmological perturbations have not yet been tested for  $f(\mathcal{R})$  gravity, and the designer model discussed here perfectly suits this purpose. As we will show in Sec. III B 2, the constraints we obtain in this work using CMB temperature and polarization anisotropy data are in perfect agreement with existent (and expected) constraints on  $G_{\text{eff}}$  considering the same effects [36].

### B. Linear perturbations in $f(\mathcal{R})$ gravity

We briefly review the main aspects concerning the evolution of linear perturbations in the hybrid metric-Palatini theory. For the full set of linearly perturbed Einstein and scalar field equations we direct the reader to Ref. [33]. Typically for modified gravity theories (however, see Refs. [17,37]), the hybrid metric-Palatini theory introduces a nonzero slip between the gravitational potentials in the Newtonian gauge,  $\Phi = \delta g_{00}/(2g_{00})$  and  $\Psi = -\delta g_{ii}/(2g_{ii})$ . Neglecting any anisotropic contribution from matter fields, the anisotropy equation becomes

$$\Phi - \Psi = \frac{\delta f_{\mathcal{R}}}{1 + f_{\mathcal{R}}}, \quad (10)$$

where  $\delta f_{\mathcal{R}}$  is the linear perturbation of the scalar field with its background value denoted by  $f_{\mathcal{R}}$ . The evolution of  $\delta f_{\mathcal{R}}$  is dictated by the linear perturbation of the scalar field equation of motion,

$$\begin{aligned} \delta \ddot{f}_{\mathcal{R}} + \delta \dot{f}_{\mathcal{R}} \left( 2\mathcal{H} - \frac{\dot{f}_{\mathcal{R}}}{f_{\mathcal{R}}} \right) \\ + \delta f_{\mathcal{R}} \left( k^2 + \frac{\dot{f}_{\mathcal{R}}^2}{2f_{\mathcal{R}}^2} + a^2 m_{f_{\mathcal{R}}}^2 - \frac{\kappa^2}{3} a^2 T \right) \\ + \Psi \left( \frac{\dot{f}_{\mathcal{R}}^2}{f_{\mathcal{R}}} - 2\dot{f}_{\mathcal{R}} - 4\dot{f}_{\mathcal{R}} \mathcal{H} \right) \\ - \dot{f}_{\mathcal{R}} (3\dot{\Phi} + \dot{\Psi}) = \frac{f_{\mathcal{R}}}{3} a^2 \kappa^2 \delta T, \end{aligned} \quad (11)$$

where  $\delta T$  denotes the linear perturbation of the trace of the stress-energy tensor,  $T = -\rho + 3p$ , and for this equation only, dots indicate derivatives with respect to conformal time  $\tau$  with  $dt = a d\tau$ , and  $\mathcal{H} \equiv aH$ .

It has been shown in Ref. [33] that the evolution of  $\delta f_{\mathcal{R}}$  is characterized by quick oscillations around zero, which end up reflecting in the ratio between the Newtonian

potentials,  $\gamma \equiv \Phi/\Psi$ . These oscillations are scale dependent, oscillating faster and with larger amplitude at smaller scales. They can produce noticeable oscillations at near-horizon scales, depending on the initial value of the scalar field at early times that, for instance, have an impact on the Poisson equation. Due to the Hubble friction term [see Eq. (11)], these modifications eventually get damped as one approaches  $a \approx 1$ , becoming negligible at the present with no signs of significant subhorizon modifications.

We will explore the behavior of  $\delta f_{\mathcal{R}}$  further in Secs. II B 1 and II B 2, focusing on its subhorizon and early-time evolution, respectively, where we will develop accurate approximations for these regimes. In order to test our approximations, we follow Ref. [33] and solve the exact numerical evolution of the gravitational potentials and  $\delta f_{\mathcal{R}}$ , using the linearly perturbed conservation equations for the stress-energy tensor and the first-order differential equations for the lensing potential,  $\Phi_+ \equiv (\Phi + \Psi)/2$ .

#### 1. Subhorizon approximation

We first consider wave modes that are deep within the Hubble radius with wave number  $k \gg aH$ . To describe this limit, we adopt the quasistatic approximation, discarding time derivatives of perturbations when compared to their spatial variation. Generally, for Horndeski scalar-tensor theories, this is a good approximation on small scales [38]. In practice, this allows one to keep the terms proportional to  $k^2/(a^2 H^2)$  as well as those related to the matter perturbation  $\delta \rho_m$  and the scalar field effective mass  $m_{f_{\mathcal{R}}}^2$ . The latter sets a modified length scale that can be compared to that of the perturbations.

From the 0–0 linearly perturbed Einstein equation in the Newtonian gauge, we obtain in the subhorizon regime [33]

$$\frac{k^2}{a^2} \Phi \approx \frac{1}{2(1 + f_{\mathcal{R}})} \left[ \delta f_{\mathcal{R}} \left( \frac{k^2}{a^2} \right) - \kappa^2 \delta \rho_m \right], \quad (12)$$

where  $\delta \rho_m \equiv \rho_m \delta_m$ . Using this approximation in the anisotropy equation we then get

$$\frac{k^2}{a^2} \Psi \approx -\frac{1}{2(1 + f_{\mathcal{R}})} \left[ \delta f_{\mathcal{R}} \left( \frac{k^2}{a^2} \right) + \kappa^2 \delta \rho_m \right]. \quad (13)$$

One can then calculate a similar approximation for  $\delta f_{\mathcal{R}}$  from Eq. (11),

$$\delta f_{\mathcal{R}} \approx -\frac{H_0^2 E_m}{k^2/a^2 + m_{f_{\mathcal{R}}}^2} f_{\mathcal{R}} \delta_m, \quad (14)$$

which can be inserted back into Eqs. (12) and (13) such that

$$\frac{k^2}{a^2} \Phi \approx -\frac{H_0^2 E_m \delta_m}{2(1 + f_{\mathcal{R}})} \left[ \frac{k^2/a^2 (f_{\mathcal{R}} + 3) + 3m_{f_{\mathcal{R}}}^2}{k^2/a^2 + m_{f_{\mathcal{R}}}^2} \right], \quad (15)$$

$$\frac{k^2}{a^2} \Psi \approx -\frac{H_0^2 E_m \delta_m}{2(1+f_{\mathcal{R}})} \left[ \frac{k^2/a^2(3-f_{\mathcal{R}}) + 3m_{f_{\mathcal{R}}}^2}{k^2/a^2 + m_{f_{\mathcal{R}}}^2} \right], \quad (16)$$

where  $E_m \equiv \Omega_m a^{-3}$ .

These approximations can, in turn, be used to obtain an expression for the lensing potential,  $\Phi_+$ , in this regime:

$$\frac{k^2}{a^2} \Phi_+ \approx -\frac{3H_0^2 E_m}{2(1+f_{\mathcal{R}})} \delta_m, \quad (17)$$

whereas the slip between the potentials,  $\delta f_{\mathcal{R}}$ , is given by

$$\delta f_{\mathcal{R}} \approx \frac{2k^2}{3a^2} \frac{f_{\mathcal{R}} \Phi_+}{k^2/a^2 + m_{f_{\mathcal{R}}}^2}. \quad (18)$$

As mentioned in Sec. I, the background value of the scalar field is required to be small in order for the metric-Palatini theory to avoid Solar System tests. In these circumstances, the quasistatic modifications will be almost unnoticeable, even if the range of the modifications, given by the effective Compton wavelength  $\lambda_C = 2\pi/m_{f_{\mathcal{R}}}$ , is relevant. For instance, note that for  $f_{\mathcal{R}} \rightarrow 0$ ,  $\delta f_{\mathcal{R}} \rightarrow 0$  since  $\delta f_{\mathcal{R}}$  is proportional to the background value of the

scalar field  $f_{\mathcal{R}}$  in the quasistatic regime, as can be seen in Eq. (18).

The  $f(\mathcal{R})$  models that have been analyzed so far [33,34] evolve toward smaller deviations from  $\Lambda$ CDM as we approach the present, with  $f_{\mathcal{R}}$  tending to negligible values. This renders the modifications in the quasistatic regime subdominant, as was explicitly shown in Ref. [33] for the designer  $f(\mathcal{R})$  model, with no mentionable enhancement of the perturbations in this regime when compared to  $\Lambda$ CDM.

In Fig. 2 we compare the numerical evolution of the ratio between the Newtonian potentials,  $\gamma$ , with its quasistatic approximation,

$$\gamma_{\text{QS}} \equiv \frac{\Phi}{\Psi} = \frac{k^2/a^2(3+f_{\mathcal{R}}) + 3m_{f_{\mathcal{R}}}^2}{k^2/a^2(3-f_{\mathcal{R}}) + 3m_{f_{\mathcal{R}}}^2}. \quad (19)$$

We see that it is an accurate approximation at late times, as a consequence of large  $k/(aH)$  values. As we approach the present time in our models, the subhorizon modifications become suppressed, leading in turn to a very small difference between the compared values. This accuracy holds even when we consider larger initial values for the scalar field,  $f_{\mathcal{R}i}$ .

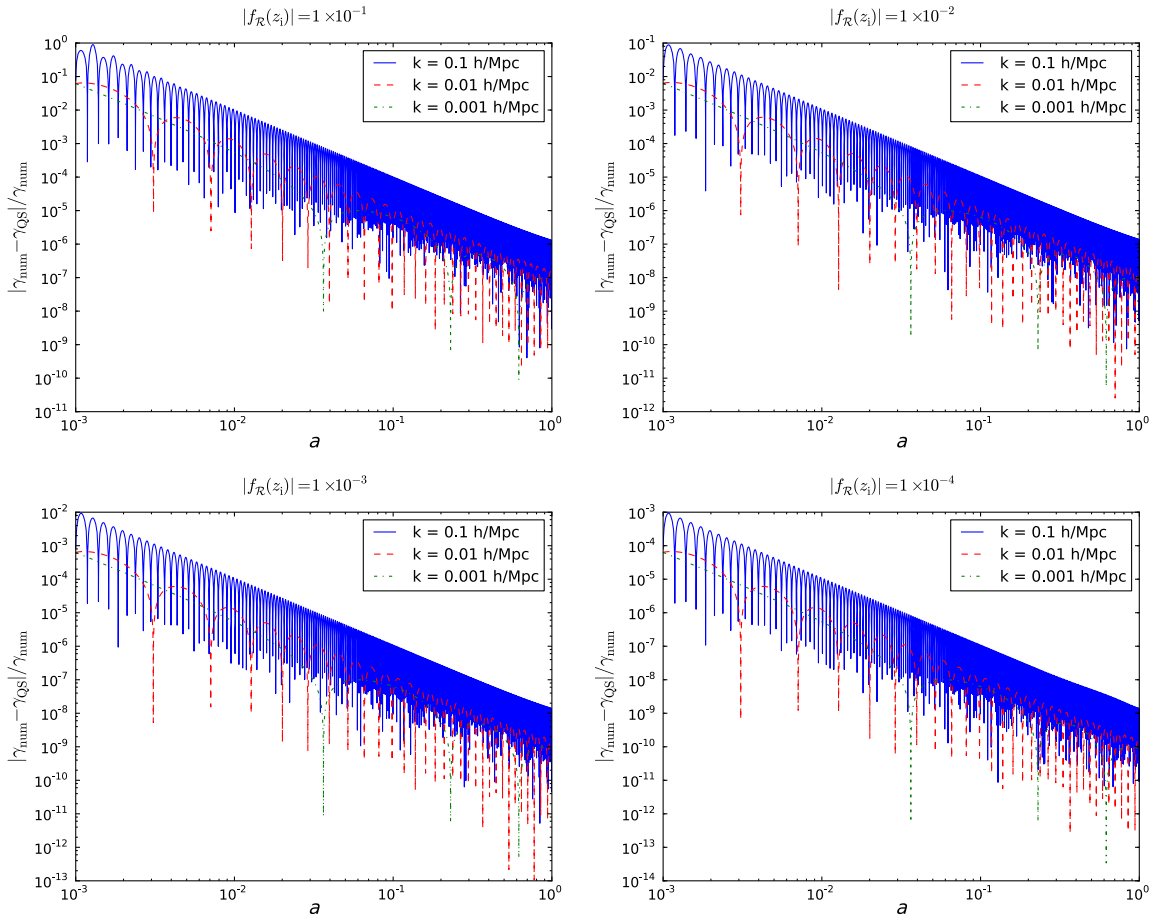


FIG. 2. Relative difference  $|\gamma_{\text{num}} - \gamma_{\text{QS}}|/\gamma_{\text{num}}$  between the numerical ratio  $\gamma \equiv \Phi/\Psi$  and its quasistatic (QS) approximation given by Eq. (19). We have considered  $z_i = 1000$  and fixed  $\Omega_m = 0.30$ .

However, the quasistatic approximation breaks down at earlier times for the smaller scales, due to the oscillatory behavior of  $\delta f_{\mathcal{R}}$  discussed in Sec. II B. For large initial values of the scalar field the error can be of order unity and decreases as we consider smaller values for  $f_{\mathcal{R}i}$ . Hence, for an accurate but computationally efficient description of the evolution of  $\gamma$  in the designer  $f(\mathcal{R})$  model that is valid across a large range of redshifts and scales, some corrections must be applied to the subhorizon approximation (see Sec. III B 2).

Lastly, we emphasize that in the hybrid metric-Palatini model,  $f_{\mathcal{R}}$  and  $\delta f_{\mathcal{R}}$  are strongly suppressed at the present, and  $(G_{\text{eff}} - G)/G \ll 1$  at any scale, consistent with Solar System tests. In contrast, in metric  $f(R)$  gravity, for modes well within the Compton radius, we have  $(G_{\text{eff}} - G)/G = 4/3$  at linear order, and the model needs to employ a nonlinear chameleon mechanism [39–42] to restore  $G_{\text{eff}}/G \rightarrow 1$  at the small scales probed by Solar System tests. Unlike the chameleon mechanism, however, the suppression in the hybrid metric-Palatini model is independent of environment and cannot be tested by unscreened small objects in voids [24] or unscreened by environment-dependent statistical measurements of the large-scale structure [25]. We recall that it is for this aspect that we adopt the decaying early-time gravitational modification characterized by the hybrid metric-Palatini model rather than the decaying mode of metric  $f(R)$  gravity, where an effective 4/3 enhancement of the gravitational coupling at late times would always be present at some level.

## 2. Early-time corrections

The dynamics of  $\delta f_{\mathcal{R}}$  is dictated by Eq. (11), which is the equation of a damped harmonic oscillator with a driving force proportional to the matter perturbation. The frequency of the oscillation depends on the mode wave number  $k$ , while the damping term is dominated by the Hubble parameter at early times, and  $\delta f_{\mathcal{R}}$  quickly becomes negligible toward late times, where the oscillations are no longer observable. The driving term could deviate the equilibrium position of the oscillations. However, note that it is proportional to  $f_{\mathcal{R}}$ , which not only is fixed to a small value at early times as we study small deviations from GR, but also evolves toward zero at late times, rendering the external force term almost negligible.

Hence, rewriting Eq. (11) to depend on  $\ln a$ , assuming  $\dot{f}_{\mathcal{R}}, \ddot{f}_{\mathcal{R}} \ll 1$ , but not neglecting terms proportional to  $\dot{f}_{\mathcal{R}}/f_{\mathcal{R}}$ , we approximate it to

$$\delta f_{\mathcal{R}}'' + \delta f_{\mathcal{R}} \left( \frac{k^2}{a^2 H^2} + \frac{f_{\mathcal{R}}'}{2f_{\mathcal{R}}^2} + \frac{H_0^2 \Omega_m a^{-3}}{H^2} \right) + \delta f_{\mathcal{R}}' \left( 3 + \frac{H'}{H} - \frac{f_{\mathcal{R}}'}{f_{\mathcal{R}}} \right) \approx 0, \quad (20)$$

for which we attempt a solution under the Wentzel-Kramers-Brillouin approximation given by

$$\delta f_{\mathcal{R}} \approx \frac{A}{\sqrt{2w}} a^{-\gamma_{\text{exp}}} \cos \left( \int w d \ln a + \theta_0 \right). \quad (21)$$

We expect the approximation to be valid as long as the adiabatic condition  $|\dot{w}| \ll w^2$  holds, where  $w^2$  is the term multiplying  $\delta f_{\mathcal{R}}$  in Eq. (20), and  $\gamma_{\text{exp}}$  is the quantity multiplying the  $\delta f_{\mathcal{R}}'$  term in Eq. (20). The constants  $\theta_0$  and  $A$  can be fixed by imposing suitable initial conditions for  $\delta f_{\mathcal{R}}$  and  $\delta f_{\mathcal{R}}'$  at a chosen redshift.

For the  $f(\mathcal{R})$  designer model, the ratio between  $f_{\mathcal{R}}'$  and  $f_{\mathcal{R}}$  can be easily calculated at early times using the initial conditions presented in Sec. II A. This yields

$$\frac{f_{\mathcal{R}}'}{f_{\mathcal{R}}} \approx \sqrt{d} - a_{\text{aux}}. \quad (22)$$

With this approximation, it is possible to simplify  $w$  and obtain an analytical solution for the integral  $\int w d \ln a$ . The details of this calculation may be found in Appendix B.

In Fig. 3 we set the initial conditions for  $\delta f_{\mathcal{R}}$  by determining  $\theta_0$  such that  $\delta f_{\mathcal{R}}$  is zero at the chosen initial redshift  $z_i = 1000$ . We note that this is completely arbitrary, but not particularly relevant for the overall evolution of  $\delta f_{\mathcal{R}}$  since it quickly oscillates around zero. We can then differentiate Eq. (20) with respect to  $\ln a$  and compute  $A$  by calculating the numerical value of  $\delta f_{\mathcal{R}}'$  using Eq. (67) of Ref. [33] at the same redshift.

We see in Fig. 3 that our analytical approximation works remarkably well, considering the complexity of the equation describing the dynamics of  $\delta f_{\mathcal{R}}$ . Even though it may fail in predicting the exact amplitude of the oscillations, the relative difference to the numerical results is insignificantly small compared to the precision available with current experiments. Also, it clearly encompasses the desired dependence on the scale of the modes of the perturbations, with a higher amplitude and frequency of oscillation the smaller scales (higher  $k$ ) one considers.

Lastly, Fig. 3 serves as further confirmation of the viability of the subhorizon approximations derived in Sec. II B 1 at late times. As Eq. (18) dictates,  $\delta f_{\mathcal{R}}$  should be strongly suppressed in the subhorizon regime following the behavior of the background scalar field value and with  $k \gg aH$ .

## C. Decoupling at high redshifts

The hybrid metric-Palatini modification of gravity needs to decouple at high redshifts in order not to violate stringent high-curvature constraints from the CMB. However, we wish to determine below which redshift  $z_{\text{on}}$  the modification can be introduced and to which degree a decaying early-time modification motivated by the evolution of hybrid metric-Palatini gravity at  $z \leq z_{\text{on}}$  can be constrained by the CMB radiation observed today. In order to formulate an explicit realization of the decaying early-modified

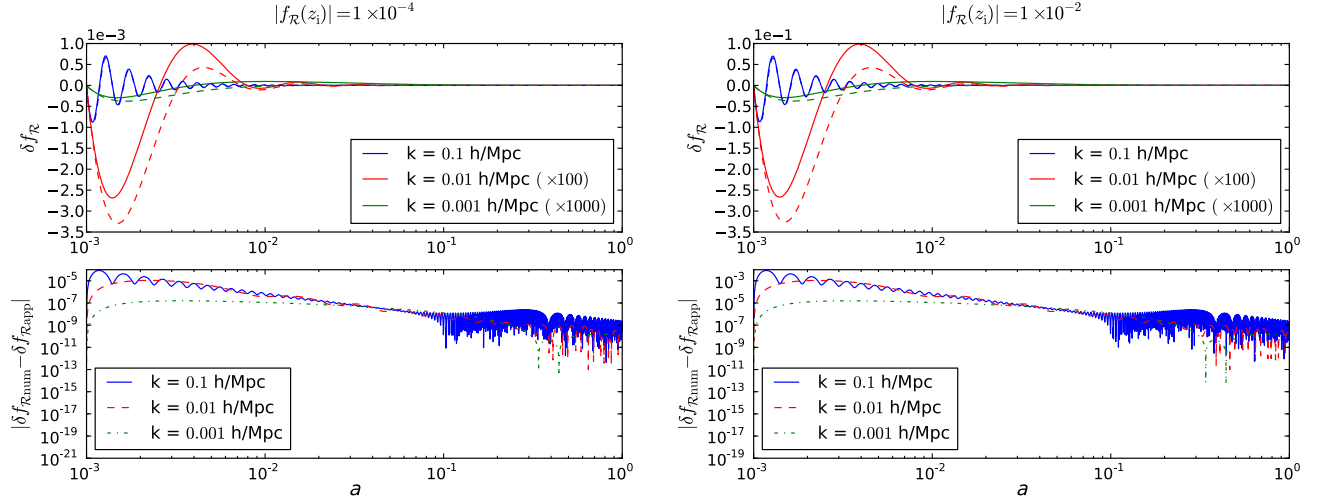


FIG. 3. (Top panels) Numerical evolution (solid lines) of the perturbation  $\delta f_{\mathcal{R}}$  against the evolution predicted by our analytical approximation (dashed lines) given by Eq. (21). The two largest scales have been enhanced by a factor of 100 and 1000 to be noticeable. (Bottom panels) The absolute difference between the analytical approximation and the numerical results. We have fixed  $\Omega_m = 0.30$ .

gravity model, we embed the designer hybrid metric-Palatini scenario with high-redshift decoupling in Horndeski scalar-tensor theory [16] using the effective field theory of cosmic acceleration (see Ref. [22] for a review).

#### D. Embedding in Horndeski gravity and effective field theory

We will now embed the designer  $f(\mathcal{R})$  model in the effective field theory of Horndeski gravity following the notation of Ref. [43]. Given the  $\Lambda$ CDM background expansion history of our designer hybrid metric-Palatini model, its modifications are fully specified by the effective parameters characterizing the linear perturbations,

$$\alpha_M = \frac{f'_{\mathcal{R}}}{1 + f_{\mathcal{R}}}, \quad \alpha_K = -\frac{3f'_{\mathcal{R}}}{2f_{\mathcal{R}}}\alpha_M, \quad \alpha_B = -\alpha_M, \quad (23)$$

where  $\alpha_M \equiv (M_*^2)'/M_*^2$  describes the running of the Planck mass  $\kappa^2 M_*^2 \equiv 1 + f_{\mathcal{R}}$ ;  $\alpha_K$  denotes the contribution of the kinetic energy of the scalar field; and  $\alpha_B$  determines the mixing of the kinetic contributions of the metric and scalar fields. The decaying early modifications of gravity constrained here are therefore realized in a Horndeski scalar-tensor model with

$$\alpha_{X,\text{model}} = \begin{cases} \alpha_X, & z \leq z_{\text{on}}, \\ 0, & z > z_{\text{on}}, \end{cases} \quad (24)$$

where the  $\alpha_X$ 's are given by Eq. (23) according to hybrid metric-Palatini gravity. Note that  $\alpha_{X,\text{model}}(z > z_{\text{on}}) = 0$  recovers a  $\Lambda$ CDM universe at high redshifts, avoiding the stringent high-curvature constraints around recombination.

Stability of the background solution of the Horndeski model with respect to the scalar mode requires [43]

$$Q_s \equiv \frac{2M_*^2 D}{(2 - \alpha_B)^2} > 0, \quad (25)$$

where

$$D \equiv \alpha_K + \frac{3}{2}\alpha_B^2 = -\frac{3(f'_{\mathcal{R}})^2}{2f_{\mathcal{R}}(1 + f_{\mathcal{R}})^2}. \quad (26)$$

With the evolution of  $f_{\mathcal{R}}$  given by hybrid metric-Palatini theory, we have

$$Q_s = \begin{cases} < 0, & \text{for } f_{\mathcal{R}} > 0, \\ > 0, & \text{for } f_{\mathcal{R}} < 0. \end{cases} \quad (27)$$

Hence, we require  $-1 < f_{\mathcal{R}} < 0$  to prevent ghost instabilities. To avoid a gradient instability or a superluminal sound speed  $c_s$  of the scalar field perturbation, we require that  $0 < c_s^2 \leq 1$ . To check this, we compute  $c_s^2$  in the hybrid metric-Palatini theory,

$$D \cdot c_s^2 = \frac{\kappa^2}{H^2(1 + f_{\mathcal{R}})} \left( \frac{4}{3}\rho_r + \rho_m \right) \left( f_{\mathcal{R}} + \frac{f'_{\mathcal{R}}}{2} \right) + \frac{\alpha_M}{2} \left( \frac{f'_{\mathcal{R}} + 2(1 + f_{\mathcal{R}})}{1 + f_{\mathcal{R}}} \right) - \frac{f''_{\mathcal{R}} - (f'_{\mathcal{R}})^2}{1 + f_{\mathcal{R}}}. \quad (28)$$

Furthermore, note that for the designer model we use in this work

$$f'_{\mathcal{R}} = \begin{cases} > 0, & \text{for } f_{\mathcal{R}} < 0, \\ < 0, & \text{for } f_{\mathcal{R}} > 0, \end{cases} \quad (29)$$

and  $|f'_{\mathcal{R}}| \gg |f_{\mathcal{R}}|$ . Therefore, for  $f_{\mathcal{R}} < 0$ ,  $f_{\mathcal{R}} + f'_{\mathcal{R}}/2 > 0$ . Also,  $f''_{\mathcal{R}}$  will be negative definite [as can be verified by differentiating Eq. (9)] for negative values of the scalar field. All of this, in conjunction with the fact that  $\alpha_M > 0$  and  $D > 0$ , ensures that  $c_s^2 > 0$  for  $-1 < f_{\mathcal{R}} < 0$ . We have also confirmed numerically that  $c_s$  is subluminal for the range of values we consider for  $f_{\mathcal{R}i}$ . Note that whereas the condition for avoiding ghost instabilities applies to all hybrid metric-Palatini gravity models and should be respected when designing any other  $f(\mathcal{R})$  models, the condition for avoiding gradient instabilities may be model dependent and should be studied in more detail for other choices of  $f(\mathcal{R})$ . For completeness, we also verify the stability of tensor modes [43] with  $Q_T \propto \kappa^2 M_*^2 = 1 + f_{\mathcal{R}} > 0$  whenever  $f_{\mathcal{R}} > -1$ . Also note that in  $f(\mathcal{R})$  models, the propagation speed of gravitational waves equals the speed of light  $c_T = 1$ .

### III. OBSERVATIONAL CONSTRAINTS

Having fully specified a theoretically consistent decaying early modified gravity model in Sec. II, we now determine the observational effects and constraints that can be set on early gravitational modifications with current cosmological data (Sec. III B). We also provide an outlook of constraints achievable with future surveys (Sec. III C).

#### A. Cosmological observables

To constrain our model parameters, we perform a Markov-chain Monte Carlo (MCMC) search using a range of geometric probes and CMB measurements by Planck 2015.

##### 1. Geometric probes

The comparison between the luminosity magnitudes of high-redshift to low-redshift supernovae type Ia (SNe Ia) provides a relative distance measure affected by the Universe's expansion rate. Complementary absolute distance measures are obtained from measuring the local Hubble constant  $H_0$  and the baryon acoustic oscillations (BAOs) in the clustering of galaxies. These probes constrain the cosmological background evolution and since the  $f(\mathcal{R})$  models considered here are designed to match the  $\Lambda$ CDM expansion history, they only serve to constrain the standard cosmological parameters and prevent degeneracies with the effect of the additional scalar degree of freedom on the fluctuations.

##### 2. Cosmic microwave background

In addition to the geometric probes described in Sec. III A 1, the acoustic peaks in the CMB also contain information on the absolute distance to the last-scattering surface. These peaks are affected by early-time departures from GR at high curvature, i.e., in the case of  $f(\mathcal{R})$

modifications, where  $z_{\text{on}}$  is sufficiently large. Gravitational modifications can generally further manifest themselves in the CMB temperature and polarization via secondary anisotropies. For details on the numerical computation of these effects in the designer hybrid metric-Palatini model, we refer the reader to Appendix A.

In Fig. 4, we show the predictions for the CMB temperature anisotropy power spectrum (TT) for three different choices of  $z_{\text{on}}$ . Hence, we introduce the oscillations between the Newtonian potentials in distinct epochs of the cosmological evolution which in turn produces different effects in the observed power spectrum. The first immediate observation is that the later we introduce these oscillations, the less significant is their impact on the TT power spectrum. This is mainly due to the fact that, at later epochs, the amplitude of the oscillations has already been considerably damped out, reducing their effect on the TT power spectrum.

The second noticeable modification of the spectrum is in the Sachs-Wolfe plateau, on scales around  $l < 100$ , where we observe a shift toward higher or smaller values compared to  $\Lambda$ CDM. The Sachs-Wolfe effect, resulting from a combination of gravitational redshift and intrinsic temperature fluctuations at angular last scattering, can lead to a variation of the temperature power spectrum like [44]

$$\frac{\Delta T}{T} \propto \delta\Phi, \quad (30)$$

where  $\delta\Phi$  corresponds to the variation of the gravitational potential  $\Phi$ . The designer hybrid metric-Palatini model introduces modifications close to the surface of last scattering. Therefore, depending on the redshift we choose

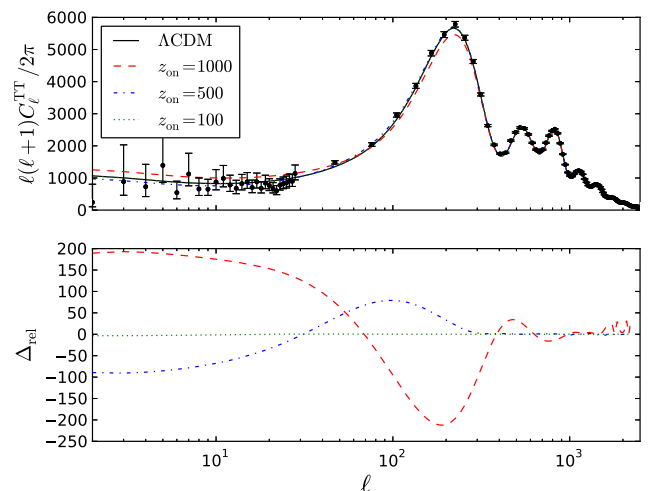


FIG. 4. (Top panel) Lensed CMB temperature anisotropy power spectrum predicted by the designer hybrid metric-Palatini model for  $|f_{\mathcal{R}}(z_i)| = 5 \times 10^{-2}$  and different values of  $z_{\text{on}}$  as well as the prediction for the  $\Lambda$ CDM model. (Lower panel) Difference from  $\Lambda$ CDM,  $\Delta_{\text{rel}} = \ell(\ell + 1)(C_\ell^{\text{TT,hybrid}} - C_\ell^{\text{TT},\Lambda})/(2\pi)$ .



to start the oscillations, the Newtonian potential  $\Phi$  will be displaced toward larger or smaller values compared to  $\Lambda$ CDM, leading to the shift we observe in the power spectrum. Then, at low  $\ell$ , we have the traditional increase in power due to the integrated Sachs-Wolfe (ISW) effect in the presence of late-time dark energy. Our model clearly mimics  $\Lambda$ CDM due to the fact that we fix the background evolution to match the standard cosmological scenario, even if the power can be deviated toward lower or smaller values due to the Sachs-Wolfe effect discussed before.

Lastly, we have what is probably the most discerning effect on the CMB TT power spectrum. When we introduce the oscillations at  $z_{\text{on}} = 1000$ , we notice a significant decrease in the amplitude of the first peak. Traditionally, at early times, the non-negligible presence of radiation after the epoch of last scattering can cause a decay of the gravitational potentials before these become constant, contributing to an early ISW effect that can influence the amplitude and position of the peaks. Therefore, if we allow modified gravity to be relevant close to the epoch of recombination, we not only modify this decay but also cause additional variation, influencing the acoustic phenomenology of the CMB. Of course, as we test lower values of  $z_{\text{on}}$ , this effect becomes increasingly negligible.

## B. Cosmological constraints

Before presenting the current cosmological constraints on decaying early modified gravity, we briefly describe the cosmological data sets we use in our analysis. We then give an outlook on constraints that can be obtained with 21-cm surveys and gravitational wave observations.

### 1. Data sets

For the SN Ia luminosity-redshift relation, we use the data set compiled in the Joint Lightcurve Analysis [45]. This includes records from the full three years of the Sloan Digital Sky Survey (SDSS) survey plus the ‘‘C11 compilation’’ assembled by Conley *et al.* [46]; comprising supernovae from the Supernovae Legacy Survey, the Hubble Space Telescope (HST), and several nearby experiments. This whole sample consists of 740 SNe Ia.

For  $H_0$ , we include information provided by the Wide Field Camera 3 on HST. The objective of this project was to determine the Hubble constant from optical and infrared observations of over 600 Cepheid variables in the host galaxies of eight SNe Ia, which provide the calibration for a magnitude-redshift relation based on 240 SNe Ia [47]. Hence, we use the Gaussian prior of  $H_0 = 73.8 \pm 2.4 \text{ km s}^{-1} \text{ Mpc}^{-1}$ .

We also use the BAO observations from the 6dF Galaxy Redshift Survey at low redshift  $z_{\text{eff}} = 0.106$  [48], as well as Data Release 7 main galaxy sample from SDSS at  $z_{\text{eff}} = 0.15$ , from the value-added galaxy catalogs hosted by New York University (NYU-VAGC) [49] and the BAO

TABLE I. Current constraints (95% C.L.) on  $f_{\mathcal{R}}(z_i = 1000)$  from the combination of surveys discussed in Sec. III B 1. Note that models with a positive sign of  $f_{\mathcal{R}}$  suffer from a ghost instability (see Sec. II D) and models with  $z_{\text{on}} = 100$  cannot be constrained within the prior  $|f_{\mathcal{R}i}| < 0.1$  required for the viability of the approximations performed in Sec. II B 2. However, a constraint of  $|f_{\mathcal{R}i}| \lesssim 10^{-3}$  on all models will be achievable with 21-cm intensity mapping (see Sec. III C). We also present constraints on the value of  $f_{\mathcal{R}}$  at the redshift of decoupling,  $z_{\text{on}}$ , and at the present time,  $z = 0$ .

$z_{\text{on}}$	$\text{sgn}(f_{\mathcal{R}})$	$ f_{\mathcal{R}i}  \equiv  f_{\mathcal{R}}(z_i) $	$ f_{\mathcal{R}}(z_{\text{on}}) $	$ f_{\mathcal{R}}(z = 0) $
1000	$\pm$	$< 1.3 \times 10^{-2}$	$< 1.3 \times 10^{-2}$	$< 1.3 \times 10^{-8}$
500	$\pm$	$< 4.7 \times 10^{-2}$	$< 1.2 \times 10^{-2}$	$< 4.7 \times 10^{-8}$
100	$\pm$	...	...	...
1000	...	$< 1.1 \times 10^{-2}$	$< 1.1 \times 10^{-2}$	$< 1.1 \times 10^{-8}$
500	...	$< 4.8 \times 10^{-2}$	$< 1.2 \times 10^{-2}$	$< 4.8 \times 10^{-8}$
100	...	...	...	...

signal from the Baryon Oscillation Spectroscopic Survey Data Release 11 at  $z_{\text{eff}} = 0.57$  [50].

Lastly, we use the Planck 2015 data for the CMB. The Planck temperature and polarization and Planck lensing likelihood codes may be found in the Planck Legacy Archive [51].

### 2. Constraints

Using the data sets described in Sec. III B 1, we conduct a MCMC parameter estimation analysis with COSMOMC [52] (see Appendix A for details). We summarize our constraints on the early-time decaying modified gravity model of Sec. II in Table I. It is easily noticeable that the constraining power of the data over the model changes significantly the later we introduce the oscillations between the Newtonian potentials ( $z \leq z_{\text{on}}$ ).

For  $z_{\text{on}} = 1000$ , allowing both signs for  $f_{\mathcal{R}i} \equiv f_{\mathcal{R}}(z_i = 1000)$ , we infer a one-dimensional-marginalized constraint of  $|f_{\mathcal{R}i}| < 1.3 \times 10^{-2}$  (95% C.L.), where we adopt a flat symmetric prior  $f_{\mathcal{R}i} \in [-0.1, 0.1]$ . We stress, however, that positive values of  $f_{\mathcal{R}i}$  are affected by the ghost instability discussed in Sec. II D. Considering the stable branch only with a negative flat prior, we find  $|f_{\mathcal{R}i}| < 1.1 \times 10^{-2}$ . These values are comparable to the constraints obtained in Ref. [34] on  $f(\mathcal{R})$  models that deviate from the  $\Lambda$ CDM expansion history, using background data alone. Although we note that these constraints have been inferred for initial modifications at much higher redshift,  $\Lambda$ CDM is clearly the favored model and we find no evidence for early-time modifications in the observations. The constraints we found are mostly driven by two prominent effects on the CMB that we have observed in Sec. III A 2: a modification of the Sachs-Wolfe plateau and of the amplitude of the first peak. However, there is also a non-negligible contribution of CMB lensing, which is sensitive to percent-level modifications at high  $\ell$  [53]

and can constrain the effects of  $z_{\text{on}} = 1000$  shown in Fig. 4. We also note that the present absolute value of the scalar field,  $|f_{\mathcal{R}0}| \equiv |f_{\mathcal{R}}(z=0)|$ , is very small and of order  $10^{-8}$ . This implies that modifications are strongly suppressed at the smallest scales, where these are proportional to the background value of the scalar field [26] (see Sec. II B).

Finally, decreasing  $z_{\text{on}}$  leads to a considerable weakening of the constraints on the early-time deviation from GR. With  $z_{\text{on}} = 500$ , constraints on the scalar field value at equal redshift weaken by a factor of approximately 4. For  $z_{\text{on}} = 100$ , we can no longer constrain the scalar field value within the prior  $|f_{\mathcal{R}i}| < 0.1$ . This is due to the oscillations on the slip between the gravitational potentials being significantly damped out by  $z = 100$ , hence only introducing very small deviations from GR.

### C. Outlook: 21-cm and gravitational waves

Finally, we provide rough estimates of the constraints on early decaying modified gravity that will be achievable with 21-cm intensity mapping [54–56] and standard sirens [17,57,58] using gravitational waves emitted by events at cosmological distances. To estimate constraints obtainable with 21-cm surveys, we compare deviations in the matter power spectrum between the model and  $\Lambda$ CDM to bounds on modified gravity reported in Ref. [55] at  $z = 11$  and Ref. [56] at  $z = 2.5$ . We find that  $|f_{\mathcal{R}i}| \lesssim 10^{-3}$  and  $|f_{\mathcal{R}i}| \lesssim 5 \times 10^{-2}$  for  $z_{\text{on}} = 1000$ , which is competitive with the CMB constraints in Table I. Standard sirens will constrain the luminosity distance at  $z \sim (1-2)$  at the  $\sim 1\%$  level, and at the  $\sim 10\%$  level for  $z \sim 7$  [59,60]. In modified gravity models, this constraint can be used to set a bound on the evolution of the Planck mass [17], which for our model corresponds to a constraint of  $|f_{\mathcal{R}i}| \lesssim 10^3$ , which will not be competitive with the constraints in Table I.

## IV. CONCLUSIONS

In this work we explore the current cosmological constraints that can be inferred on modifications of gravity which may become significant at early times after recombination and decay toward the present. We choose the designer hybrid metric-Palatini model as a specific example of an early-time modification of gravity. Fixing the background evolution to exactly match  $\Lambda$ CDM, we are able to separate background constraints from constraints inferred from the modified dynamics of linear perturbations due to the impact that these have on the CMB. We also describe how this model can be realized in the more general context of the effective field theory formalism of Horndeski gravity, and study its stability. We conclude that the model is stable as long as the additional scalar degree of freedom introduced by the hybrid metric-Palatini theory remains negative

with an amplitude smaller than unity, which implies an effective enhancement of the gravitational coupling.

In order to perform efficient numerical computations, we develop an approximation for the evolution of the slip between the Newtonian potentials that is valid beyond the standard quasistatic subhorizon approximation. This extension becomes important at high redshifts, where we show that a quasistatic approach alone breaks down due to the known oscillations of the linear perturbations of the model [33].

Using a combination of observational data on the background evolution and of the CMB anisotropies, we infer constraints on the allowed early-time deviations from GR. The results we obtain are dependent on the redshift at which we introduce the oscillations in the slip between the gravitational potentials. If these are set at  $z_{\text{on}} = 1000$ , we are able to constrain the absolute deviation from GR at  $z_{\text{on}}$  to  $\lesssim 10^{-2}$  at the 95% confidence level. This result is comparable to the constraints obtained from background data alone in Ref. [34] for  $f(\mathcal{R})$  models that depart from the  $\Lambda$ CDM expansion history.

The constraints we obtain at this redshift can be attributed to noticeable effects on the CMB power spectrum. We are able to observe a substantial shift in the Sachs-Wolfe plateau due to a modification of the Newtonian potential  $\Phi$  at a time close to recombination. There is also a significant suppression of the first peak due to complementary variation of the gravitational potentials close to the epoch of recombination that, together with the non-negligible presence of radiation, contributes to an early integrated Sachs-Wolfe effect that can alter the amplitude and position of the peaks. Smaller contributions to the constraints can be attributed to CMB lensing, which is sensitive to the percent-level modifications we observe at high  $\ell$ . Finally, we find that future 21-cm survey data will significantly improve upon the CMB constraints, whereas using gravitational wave events as standard sirens will not provide competitive bounds.

## ACKNOWLEDGMENTS

We thank Andrew Liddle, Alex Hall, and Tomi Koivisto for the useful discussions and comments on this manuscript. N. A. L. acknowledges financial support from Fundação para a Ciência e a Tecnologia (FCT) through Grant No. SFRH/BD/85164/2012. V. S.-B. acknowledges funding provided by Consejo Nacional de Ciencia y Tecnología (CONACyT) and the University of Edinburgh. L. L. was supported by the Science and Technology Facilities Council (STFC) Consolidated Grant for Astronomy and Astrophysics at the University of Edinburgh and Swiss National Science Foundation (SNSF) Advanced Postdoc Mobility Fellowship No. 161058. Numerical computations were conducted on the COSMOS Shared Memory system at Department of Applied Mathematics and Theoretical Physics (DAMTP), University of Cambridge operated on behalf of the STFC DiRAC HPC

Facility. This equipment is funded by BIS National E-infrastructure Capital Grant No. ST/J005673/1 and STFC Grants No. ST/H008586/1 and No. ST/K00333X/1.

## APPENDIX A: IMPLEMENTATION IN MGCAMB

In order to compute the CMB observables, we implement our early decaying modified gravity model in the publicly available MGCAMB code [61], a modified version of the also public CAMB code [62] that allows us to study the effects of modified gravity models on the CMB through modifications of the linear equations describing the growth of perturbations. MGCAMB works by parametrizing the evolution of the gravitational potentials simply through two time- and scale-dependent functions: the ratio of the metric potentials  $\gamma(a, k) \equiv \Phi/\Psi$  and the effective modified gravitational coupling in the Poisson equation,  $\mu(a, k) = G_{\text{eff}}/G$ . The framework of MGCAMB is general enough to include possible early-time effects, hence it is well suited for testing the hybrid metric-Palatini theory. Moreover, we choose to work with MGCAMB as it allows us to use the approximations described in Secs. II B 1 and II B 2 to improve computational efficiency without loss of accuracy.

We implement our model by modifying both  $\gamma$  and  $\mu$  in the code. For  $\gamma$  we use the subhorizon approximation described in Eq. (19) and add an oscillatory term described by  $\delta f_{\mathcal{R}}$  to account for the early-time oscillations. From Ref. [33] we note that the gravitational potentials can be expressed as

$$\begin{aligned}\Phi &= \Phi_+ + \frac{\delta f_{\mathcal{R}}}{2(1+f_{\mathcal{R}})}, \\ \Psi &= \Phi_+ - \frac{\delta f_{\mathcal{R}}}{2(1+f_{\mathcal{R}})},\end{aligned}\quad (\text{A1})$$

which uses the observation that the early-time oscillations in  $\delta f_{\mathcal{R}}$  do not affect the lensing potential  $\Phi_+$  for small-enough values of the amplitude of the oscillations.  $\Phi_+$  has an approximately constant value of unity throughout the matter-dominated era. Therefore, with  $\Phi_+ \gg \delta f_{\mathcal{R}}$  one can perform a Taylor expansion on the ratio between the potentials that results in

$$\gamma = \frac{\Phi}{\Psi} \approx 1 - \frac{\delta f_{\mathcal{R}}}{(1+f_{\mathcal{R}})}.\quad (\text{A2})$$

We compare this approximation against numerical results in Fig. 5, finding good agreement between the two, at an accuracy comparable to that observed in Fig. 3 for the slip between the metric potentials. Given this result, we generalize  $\gamma_{\text{QS}}$  with the simple modification

$$\gamma_{\text{MG}} \approx \gamma_{\text{QS}} + \frac{\delta f_{\mathcal{R}}}{1+f_{\mathcal{R}}},\quad (\text{A3})$$

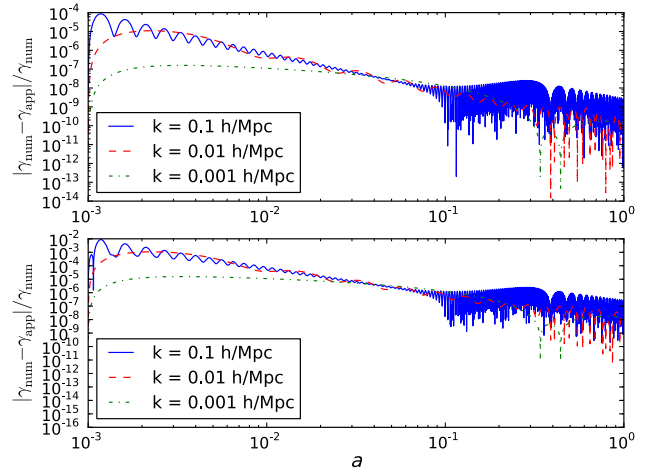


FIG. 5. Relative difference between the numerical evolution of  $\gamma \equiv \Phi/\Psi$  and the approximation in Eq. (A2). (Top panel)  $|f_{\mathcal{R}i}| = 10^{-4}$ . (Lower panel)  $|f_{\mathcal{R}i}| = 10^{-2}$ . We have again fixed  $\Omega_m = 0.30$ .

where  $\gamma_{\text{QS}}$  can be found in Eq. (19). Correspondingly, we modify  $\mu$  to include the effect of the oscillations in the Poisson equation such that

$$\mu_{\text{MG}} = \mu_{\text{QS}} + \frac{\delta f_{\mathcal{R}}}{2(1+f_{\mathcal{R}})},\quad (\text{A4})$$

where  $\mu_{\text{QS}}$  is given in Eq. (16).

Finally, note that the initial conditions required to solve for the background evolution of our models are always set at the redshift  $z_i = 1000$ . As described in Secs. II C and II D through an embedding in the effective field theory of Horndeski gravity, the model is designed to behave as  $\Lambda$ CDM at the level of linear perturbations down to a redshift  $z_{\text{on}}$ , at which point the modifications are introduced. At redshift  $z_i$  we set  $\delta f_{\mathcal{R}} = 0$ , with its subsequent evolution being determined by Eq. (21).

## APPENDIX B: ANALYTIC SOLUTION FOR THE INTEGRATED SPRING TERM

Using Eq. (22), we can simplify the  $w$  term of Eq. (21) as

$$w \approx \left[ \frac{k^2 a^{-2}}{H_0^2 E} + \frac{(a_{\text{aux}} - \sqrt{d})^2}{2} + \frac{\Omega_m}{\Omega_m + \Omega_\Lambda a^3} \right]^{1/2},\quad (\text{B1})$$

where we have neglected the presence of radiation in the Hubble factor  $H \equiv H_0 \sqrt{E}$  since applying this approximation only for redshifts deep within the matter-dominated era. For  $k \gg aH$ , Eq. (B1) can be further approximated by

$$w \approx \left( \frac{k^2}{a^2 H_0^2 E} \right)^{1/2} \left( 1 + \frac{b a^2 H_0^2 E}{2k^2} \right), \quad (\text{B2})$$

where  $b = (a_{\text{aux}} - \sqrt{d})^2/2 + \Omega_m/(\Omega_m + \Omega_\Lambda a^3)$ , which allows us to perform an analytic integration of Eq. (21). The result depends on hypergeometric functions that can, however, be approximated as unity. For simplicity, we therefore present the result without the presence of these functions:

$$\int w d \ln a \approx 2 \left( \frac{k^2 a}{H_0^2 \Omega_m} \right)^{1/2} + \frac{[a_{\text{aux}} - \sqrt{d}]^2}{4} \left( \frac{\Omega_m H_0^2}{k^2 a} \right)^{1/2} \times \left( \sqrt{\frac{\Omega_m}{\Omega_\Lambda} a^3 + 1} - 3 \right) - \Omega_m \left( \frac{H_0^2}{k^2 a} \right)^{1/2}. \quad (\text{B3})$$

In the limit of  $k \ll aH$ , we can instead approximate  $w$  as

$$w \approx \sqrt{b} \left( 1 + \frac{1}{2} \frac{k^2}{a^2 H_0^2 E b} \right). \quad (\text{B4})$$

To perform an analytic integration, we use the approximation  $b \approx (a_{\text{aux}} - \sqrt{d})^2/2 + 1$ , which results in

$$\int w d \ln a \approx \sqrt{b} + \frac{1}{2\sqrt{b}} \frac{k^2 a}{H_0^2 \Omega_m}. \quad (\text{B5})$$

We compare the implementation of the approximations in Eqs. (wappsamllk) and (B5) against numerical results in Fig. 3, finding good agreement between the two.

- 
- [1] T. Clifton, P. G. Ferreira, A. Padilla, and C. Skordis, *Phys. Rep.* **513**, 1 (2012).
- [2] K. Koyama, *Rep. Prog. Phys.* **79**, 046902 (2016).
- [3] A. Joyce, L. Lombriser, and F. Schmidt, *Annu. Rev. Nucl. Part. Sci.* **66**, annurev-nucl-102115-044553 (2016).
- [4] T. Abbott *et al.* (Dark Energy Survey Collaboration), arXiv: astro-ph/0510346.
- [5] K. S. Dawson *et al.*, *Astron. J.* **151**, 44 (2016).
- [6] R. Laureijs *et al.*, European Space Agency Report No. ESA/SRE(2011)12, 2011.
- [7] A. G. Riess *et al.*, *Astron. J.* **116**, 1009 (1998).
- [8] S. Perlmutter *et al.*, *Astrophys. J.* **517**, 565 (1999).
- [9] A. G. Riess *et al.*, *Astrophys. J.* **659**, 98 (2007).
- [10] R. Amanullah *et al.*, *Astrophys. J.* **716**, 712 (2010).
- [11] T. Padmanabhan, *Phys. Rep.* **380**, 235 (2003).
- [12] L. Lombriser and N. A. Lima, arXiv:1602.07670.
- [13] C. H. Brans and R. H. Dicke, *Phys. Rev.* **124**, 925 (1961).
- [14] A. Nicolis, R. Rattazzi, and E. Trincherini, *Phys. Rev. D* **79**, 064036 (2009).
- [15] T. P. Sotiriou and V. Faraoni, *Rev. Mod. Phys.* **82**, 451 (2010).
- [16] G. W. Horndeski, *Int. J. Theor. Phys.* **10**, 363 (1974).
- [17] L. Lombriser and A. Taylor, *J. Cosmol. Astropart. Phys.* **03** (2016) 031.
- [18] L. Lombriser, *Phys. Rev. D* **83**, 063519 (2011).
- [19] P. Brax, C. van de Bruck, S. Clesse, A.-C. Davis, and G. Sculthorpe, *Phys. Rev. D* **89**, 123507 (2014).
- [20] K. Kohri, Y. Oyama, T. Sekiguchi, and T. Takahashi, arXiv:1608.01601.
- [21] M. G. Santos *et al.*, arXiv:1501.03989.
- [22] J. Gleyzes, D. Langlois, and F. Vernizzi, *Int. J. Mod. Phys. D* **23**, 1443010 (2014).
- [23] L. Pogosian and A. Silvestri, *Phys. Rev. D* **77**, 023503 (2008).
- [24] B. Jain and J. VanderPlas, *J. Cosmol. Astropart. Phys.* **10** (2011) 032.
- [25] L. Lombriser, F. Simpson, and A. Mead, *Phys. Rev. Lett.* **114**, 251101 (2015).
- [26] T. Harko, T. S. Koivisto, F. S. N. Lobo, and G. J. Olmo, *Phys. Rev. D* **85**, 084016 (2012).
- [27] S. Capozziello, T. Harko, F. S. N. Lobo, and G. J. Olmo, *Int. J. Mod. Phys. D* **22**, 1342006 (2013).
- [28] S. Capozziello, T. Harko, T. S. Koivisto, F. S. N. Lobo, and G. J. Olmo, *Universe* **1**, 199 (2015).
- [29] G. J. Olmo, *Int. J. Mod. Phys. D* **20**, 413 (2011).
- [30] T. Koivisto and H. K.-Suonio, *Classical Quantum Gravity* **23**, 2355 (2006).
- [31] S. Capozziello, T. Harko, T. S. Koivisto, F. S. N. Lobo, and G. J. Olmo, *J. Cosmol. Astropart. Phys.* **04** (2013) 011.
- [32] S. Capozziello, T. Harko, T. S. Koivisto, F. S. N. Lobo, and G. J. Olmo, *J. Cosmol. Astropart. Phys.* **07** (2013) 024.
- [33] N. A. Lima, *Phys. Rev. D* **89**, 083527 (2014).
- [34] N. A. Lima and V. S.-Barreto, *Astrophys. J.* **818**, 186 (2016).
- [35] K.-i. Umezū, K. Ichiki, and M. Yahiro, *Phys. Rev. D* **72**, 044010 (2005).
- [36] S. Galli, A. Melchiorri, G. F. Smoot, and O. Zahn, *Phys. Rev. D* **80**, 023508 (2009).
- [37] L. Lombriser and A. Taylor, *Phys. Rev. Lett.* **114**, 031101 (2015).
- [38] L. Lombriser and A. Taylor, *J. Cosmol. Astropart. Phys.* **11** (2015) 040.
- [39] J. Khoury and A. Weltman, *Phys. Rev. Lett.* **93**, 171104 (2004).
- [40] W. Hu and I. Sawicki, *Phys. Rev. D* **76**, 064004 (2007).
- [41] P. Brax, C. van de Bruck, A.-C. Davis, and D. J. Shaw, *Phys. Rev. D* **78**, 104021 (2008).
- [42] L. Lombriser, *Ann. Phys. (Berlin)* **526**, 259 (2014).

- [43] E. Bellini and I. Sawicki, *J. Cosmol. Astropart. Phys.* **07** (2014) 050.
- [44] R. K. Sachs and A. M. Wolfe, *Astrophys. J.* **147**, 73 (1967).
- [45] M. Betoule *et al.*, *Astron. Astrophys.* **568**, A22 (2014).
- [46] A. Conley *et al.*, *Astrophys. J. Suppl.* **192**, 1 (2011).
- [47] A. G. Riess, L. Macri, S. Casertano, H. Lampeitl, H. C. Ferguson, A. V. Filippenko, S. W. Jha, W. Li, and R. Chornock, *Astrophys. J.* **730**, 119 (2011).
- [48] F. Beutler, C. Blake, M. Colless, D. Heath Jones, L. Staveley-Smith, L. Campbell, Q. Parker, W. Saunders, and F. Watson, *Mon. Not. R. Astron. Soc.* **416**, 3017 (2011).
- [49] A. J. Ross, L. Samushia, C. Howlett, W. J. Percival, A. Burden, and M. Manera, *Mon. Not. R. Astron. Soc.* **449**, 835 (2015).
- [50] L. Anderson *et al.*, *Mon. Not. R. Astron. Soc.* **441**, 24 (2014).
- [51] R. Adam *et al.* (Planck Collaboration), *Astron. Astrophys.* **594**, A1 (2016).
- [52] A. Lewis and S. Bridle, *Phys. Rev. D* **66**, 103511 (2002).
- [53] E. Calabrese, A. Cooray, M. Martinelli, A. Melchiorri, L. Pagano, A. Slosar, and G. F. Smoot, *Phys. Rev. D* **80**, 103516 (2009).
- [54] P. Madau, A. Meiksin, and M. J. Rees, *Astrophys. J.* **475**, 429 (1997).
- [55] P. Brax, S. Clesse, and A.-C. Davis, *J. Cosmol. Astropart. Phys.* **01** (2013) 003.
- [56] A. Hall, C. Bonvin, and A. Challinor, *Phys. Rev. D* **87**, 064026 (2013).
- [57] B. F. Schutz, *Nature (London)* **323**, 310 (1986).
- [58] D. E. Holz and S. A. Hughes, *Astrophys. J.* **629**, 15 (2005).
- [59] C. Cutler and D. E. Holz, *Phys. Rev. D* **80**, 104009 (2009).
- [60] N. Tamanini, C. Caprini, E. Barausse, A. Sesana, A. Klein, and A. Petiteau, *J. Cosmol. Astropart. Phys.* **04** (2016) 002.
- [61] A. Hojjati, L. Pogosian, and G.-B. Zhao, *J. Cosmol. Astropart. Phys.* **08** (2011) 005.
- [62] A. Lewis, A. Challinor, and A. Lasenby, *Astrophys. J.* **538**, 473 (2000).